



XIX Encontro Nacional de Tecnologia do
Ambiente Construído
ENTAC 2022

Ambiente Construído: Resiliente e Sustentável
Canela, Brasil, 9 a 11 novembro de 2022

Simulação e validação de um sistema de aquecimento solar de água com termossifão utilizando o software EnergyPlus.

Simulation and validation of a thermosyphon solar water heating system using EnergyPlus software

Vanessa Costa Santos

Universidade Estadual de Londrina | Londrina | Brasil | vanessacosta@uel.br

Guilherme Vilela Sanches

Universidade Estadual de Londrina | Londrina | Brasil | gvilela.sanches@uel.br

Thalita Giglio

Universidade Estadual de Londrina | Londrina | Brasil | thalita@uel.br

Resumo

Há uma lacuna de trabalhos que avaliam sistemas de aquecimento solar de água (SAS) por termossifão em uso. Este estudo apresenta procedimentos para modelar e validar um SAS no software EnergyPlus sob diferentes condições de utilização. O modelo do sistema foi validado comparando-o com medições obtidas em um conjunto habitacional de interesse social. Foram considerados cinco clusters que representam a diversidade de uso do sistema. Foi adotada a Raiz do Erro Quadrático Médio (RSME) entre os valores simulados e medidos. Os RSME máximos e mínimos obtidos foram de 10,26% e 4,76%, respectivamente, o que demonstra a possibilidade de utilização do EnergyPlus para simular SAS.

Palavras-chave: Energia solar térmica. Circulação Natural. Comportamento do usuário. Procedimentos.



SANTOS, V.; SANCHES, G.; GIGLIO, T. Simulação e validação de um sistema de aquecimento solar de água com termossifão utilizando o software EnergyPlus. ENTAC2022. In: ENCONTRO NACIONAL DE TECNOLOGIA DO AMBIENTE CONSTRUÍDO, 19., 2022, Canela. **Anais...** Porto Alegre: ANTAC, 2022. p. XXX-XXX.

Abstract

There is a lack of studies that consider thermosyphon solar water heating systems under operation. This study presents procedures to model and validate a thermosyphon solar water heating system simulated using EnergyPlus software under different usage conditions. The system was validated by comparing it with measurements obtained in a social housing complex. Five clusters that represent the diversity in system usage were considered. The Root Mean Square Error (RMSE) between the simulated and measured values was adopted. The maximum and minimum RMSE obtained were 10.26% and 4.76%, respectively, which demonstrate the possibility of using EnergyPlus to simulate thermosyphon solar water heating systems.

Keywords: Solar thermal energy. Natural circulation. Occupant behavior. Procedures.

INTRODUCTION

EnergyPlus and TRNSYS are widely used softwares in studies that involve computer simulations of the performance of SWHS under different configurations and usage conditions. Generally, common issues in modeling include uncertainties related to the accuracy of system specifications, simplifications or assumptions of physical processes, amount of input data, and interaction with external elements, such as climate conditions and system users' behavior [1], [2]. In addition, the gaps in computer simulation methods to specific studies, such as solar water heating, and the difficulties in managing simulation software are obstacles in reliable model construction.

Studies related to the validation of thermosyphon SWHS have been found in literature [3], [4], and [5]. [3] and [5] used TRNSYS to simulate the behavior of a SWHS with flat plate collectors, a horizontal storage tank, and natural circulation in Nicosia, Cyprus. The system was validated comparing the simulated values with measurements of a storage tank average water temperature in a monitored system. The obtained differences between the measured and simulated values were within the accuracy range of the measuring equipment. Thus, the simulated model showed similar behavior to the real system. They address the validation of SWHS with features similar to those used in Brazil, however, the studies did not consider the influence of consumption. There is a lack of studies that consider the system under usage and with natural circulation operation.

The goals of this study are to present procedures to model and validate a thermosyphon SWHS under operation using EnergyPlus software, assessing the system response in different usage conditions.

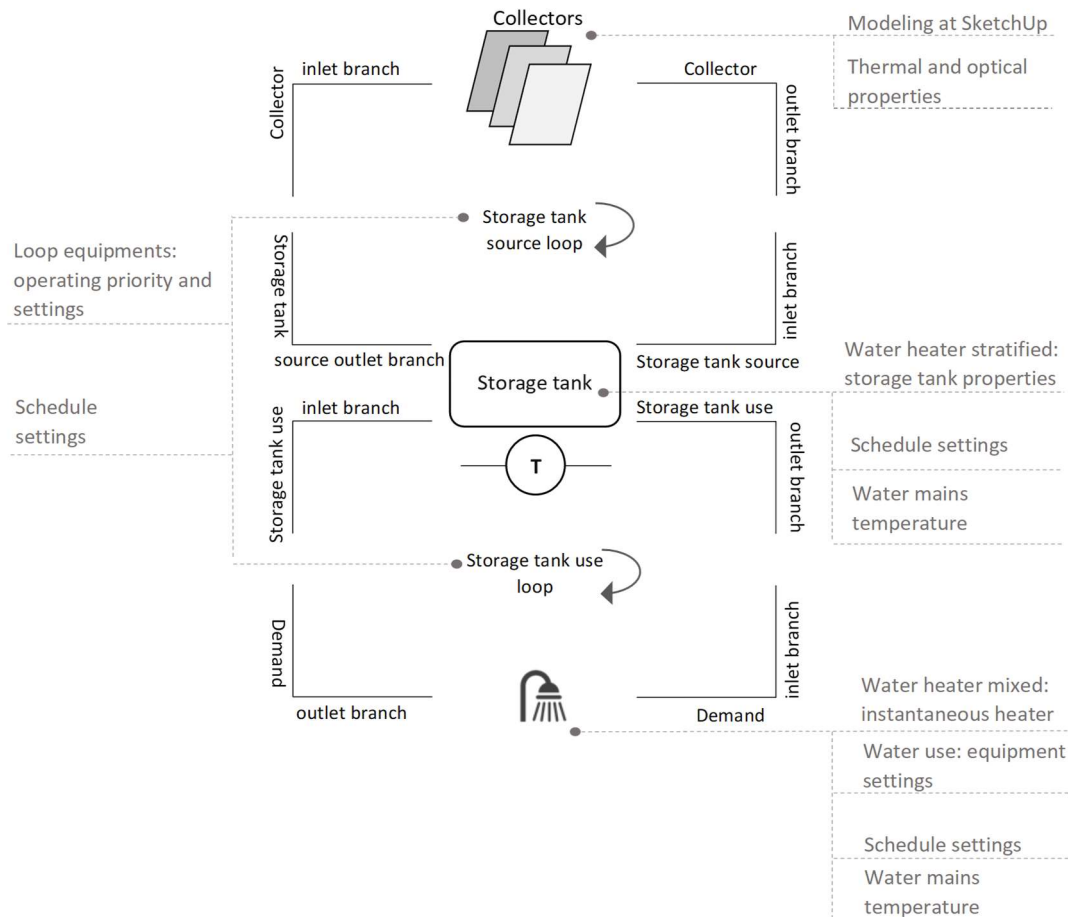
MATERIALS AND METHODS

A solar collector shaping was performed for modeling a SWHS, using SketchUp¹ software, according to the collector azimuth deviation (γ) and slope (β). The collector surface shaping file was input to EnergyPlus, version 8.8.0, to configure several objects that model a SWHS. These objects correspond with each other over a dependence link.

¹ Interface between Sketchup and EnergyPlus is created by installing a Plug-in or an extension, Euclid. Euclid creates the interface by producing a file .idf such that the model drawn in Sketchup can be interpreted correctly by EnergyPlus. Euclid's tools must be used together with SketchUp during interface creation.

The main structure modeling of a SWHS is sustained by loop settings. In this model, two plant loops occur simultaneously and interact with the storage tank, as shown in Figure 1. The first storage tank source loop comprises settings between collectors and storage tank, which the cold water, located in the lower layers of the storage tank, flows to collectors, heats, and then returns to the storage tank, thus restarting the loop. All the objects that specify both the collectors and primary circuit piping are included in this loop.

Figure 1: Schematic of the SWHS main structure model on EnergyPlus software.



Source: the author.

The second loop, storage tank use, comprises the settings between the storage tank and demand. As hot water, at the upper layers, is drained to supply the demand, the storage tank is refilled with cold water. In this loop, certain objects were configured: properties of secondary circuit piping conditions, a tempering valve to control water temperature by diverting flow, auxiliary support system, and equipment of consumption points. In this study, an instantaneous heater was used for the showerhead.

All SWHS equipment—collectors, storage tanks, pipe circuits, tempering valves, and water use equipment—are distributed throughout 13 branches, a few of which are presented in Figure 1.

The solar collector operating schedule is based on the object's settings AvailabilityManager:DifferentialThermostat that allows to compare the water temperature between two nodes of the system. This configuration was determined

empirically based on the comparison between the measured and simulated results of the final water consumption temperature.

Another object, `SolarCollectorPerformance:FlatPlate`, requests the entry of optical gain coefficient, collector plate heat loss, incident angle modifier, and mass flow rate. The solar collector efficiency (η) can be calculated using two equations: the first equation shows a linear correlation of the thermal losses ($F_R U_L$), and the second equation shows a quadratic correlation of $F_R U_L$. This study uses the linear correlation, as shown in Equation (1):

$$\eta = c_0 + c_1 \frac{(T_{in} - T_{air})}{I_{solar}} \quad (1)$$

where c_0 is the optical gain coefficient ($F_R(\tau\alpha)_n$), c_1 is the thermal loss coefficient, T_{in} is the water temperature in the collector input, T_{air} is the external air temperature, and I_{solar} is the total incident solar radiation.

To calculate the collector transmittance range for different solar radiation incident angles, a linear equation of incident modifier angle was used, expressed by (2):

$$K_{\tau\alpha} = 1 + b_0 \left(\frac{1}{\cos \theta} - 1 \right) \quad (2)$$

where $K_{\tau\alpha}$ is the incident modifier angle, b_0 is the linear coefficient of the incident angle modifier, and θ is the radiation incident angle.

Thus, in object `SolarCollectorPerformance:FlatPlate`, only the coefficients c_0 , c_1 , and b_0 were included.

In this study, the storage tank is a horizontal and stratified tank are exposed to an external environment, i.e., placed above the roof. The object `WaterHeating:Stratified` was used to establish its settings. . In addition, the water inlet and outlet heights were defined. It was assumed that the hot water entering from the collector and hot water exiting for consumption are placed 0.55 m above the bottom. The cold water inlet coming from the supply network and the water outlet that goes to the collector were placed at the bottom of the tank (0 m). The cold water temperature was determined from a monthly schedule included on the objects `Schedule:File` linked with the `Site:WaterMainsTemperature`. The stratification level of the storage tank was defined by establishing thermal losses for inner nodes or layers.

The software allows the user to configure the tank heat losses to the exposed environment—attic of a roof or external environment. In the case of exposure to external environment, hourly data of the external air temperature provided by the weather file were used.

Objects of the `WaterSystem` class were used to set up the shower flow and specify the schedules that present the bath schedules and bathing water temperature. When it is necessary to use an electric instantaneous heater as a SWHS backup, the object

WaterHeater:Mixed is used. In this model, a tempering valve was also programmed to avoid burns during usage.

VALIDATION

Modeling was validated based on certain criteria adopted from [3] and [6] to ensure its representation. The procedure consisted of comparing data from a performance indicator acquired from the measurement of a SWHS under usage, with the results of this system simulation under the same conditions. This comparison was validated from the Root Mean Square Error (RMSE) given by Equation (3), according to [6]:

$$RMSE = \sqrt{\frac{\sum_{i=1}^n [(x_{sim} - x_{meas}) / x_{meas}]^2}{n}} \quad (3)$$

where X_{sim} is the value of the performance indicator obtained by simulation, x_{meas} is the value of performance indicator obtained by measurement, and n is the total sample number. The performance indicator chosen in this validation was hot water temperature on the storage tank next to the outlet point to supply the demand. The simulation was programmed to generate output data of water temperature per minute as it was registered in the monitored SWHS measurements. Then, the average temperatures for each hour through the seven days of calibration were calculated.

DESCRIPTION OF MONITORED SYSTEM

Hot water temperature data used to validate the model were obtained from [7] and [8]. Five houses equipped with SWHSs (Figure 2a-b) were monitored over a period of one year, between April 2013 and March 2014. The houses are part of a housing complex with 1272 units located in Londrina, Brazil, whose latitude is approximately 23° (Figure 2c). Monitoring (Figure 2d-f) was realized from the installation of the temperature, water, and energy sensors distributed in strategic system points and connected to a data acquisition and real-time remote transfer system. The equipment was calibrated after the measuring period to assess its precision after a long time under operation.

Figure 2 – (a-b) Analyzed solar heating system, (c) monitored social housing complex, (d) detail of storage tank breather with consumption hot water temperature sensor inserted; (e) measured data acquisition and transmission system, and (f) flow rate and bathing water temperature sensors.



Source: the author

For data acquisition of storage tank hot water outlet temperature, one of the sensors was placed in the tank next to the consumption outlet (recorded per minute), maintaining it submerged in hot water throughout the monitoring period. Flow meters

with a sense pulse registered the bathing duration time (in minutes) and flow rate (in liters per minute). The SWHS, located on the roof above the bathroom, is composed of a single flat-plate solar collector with a gross area of 2.11 m² and a useful area of 1.94 m², without shading interference from the surroundings. The collector has an optical gain coefficient ($F_R(\tau\alpha)_n$) equal to 0.649 and thermal losses ($F_R U_L$) coefficient equal to 6.297 W/m²K.

The storage tank is placed in the external part of the roof, above the collector support quota, and has a capacity of 200 L with a specific energy loss of 0.19 kWh/month/L. The pressure-reducing box, which is responsible for cold water supply, is placed over the storage tank and has a capacity of 22 L. The houses have an instantaneous electric showerhead as a backup support.

Table 1 – Characteristics of monitored clusters

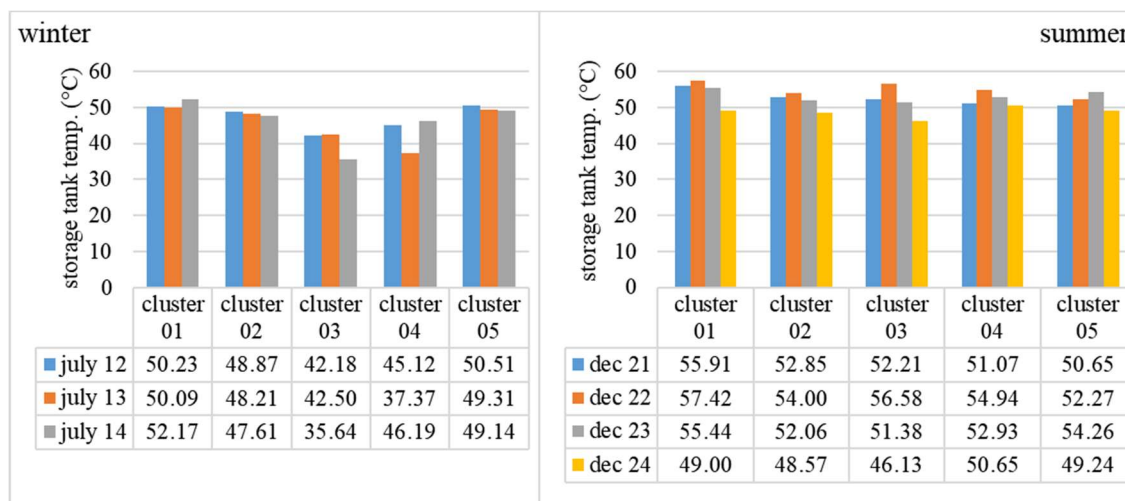
-	Cluster 01	Cluster 02	Cluster 03	Cluster 04	Cluster 05
Azimuth deviation (γ)	16°	16°	16°	16°	16°
Collector slope (β)	26.8°	44.4°	26.8°	41.5°	43.1°
Number of occupants	2	5	5	4	4

Source: the author.

SELECTION OF THE VALIDATION DAYS

In this study, we defined a range of seven days distributed in two periods during the summer and winter, aiming to observe the model's behavior in two extreme situations. Thus, validation was performed on July 12–14, 2013 and December 21–24, 2013.

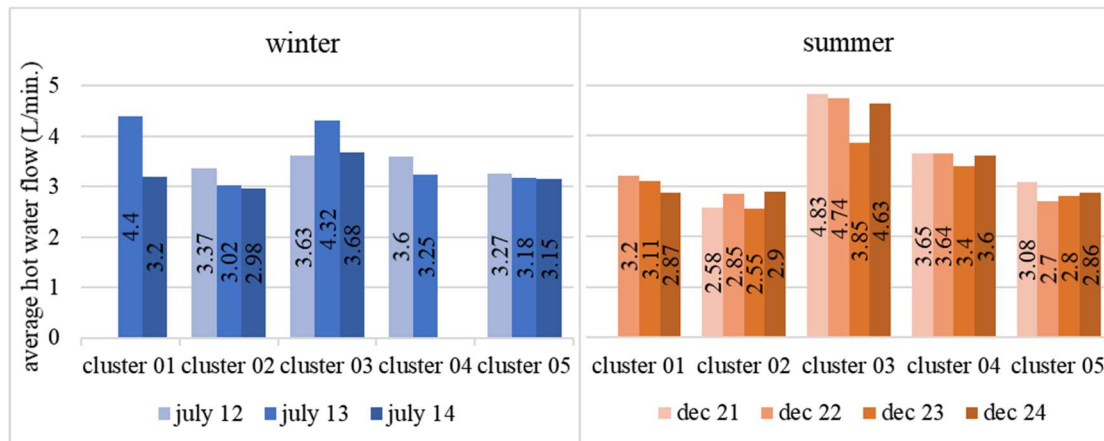
Figure 3 – Storage tank temperature measured at 0:01 a.m.



Source: the author.

The temperature values used in the simulations are shown in Figure 3. Temperatures of the cold water from the supply network obtained on a monthly average in [7], of the five clusters were 18.53 °C and 27.15 °C for July and December, respectively.

Figure 4: Daily average hot water flow used in the monitored baths



Source: the author.

Figure 4 presents the average flow of the shower observed on each monitored day for the five systems. The data in Figure 4 are limited to baths that used the solar heating system; however, certain baths with cold water have been registered during the monitoring period.

CLIMATE VARIABLES AND MODELING PARTICULARITIES

Fidelity in reproducing climate conditions is fundamental for the conformity of the performance results of a simulated system to the results of a monitored system. For the manual input of climate variables, the model underwent certain modifications. The most relevant modification was replacing the RunPeriod object with SizingPeriod:DesignDay object, which allows the manual input of several data such as solar radiation, wind speed and direction, barometric pressure, dry-bulb temperature, and criteria of humidity condition.

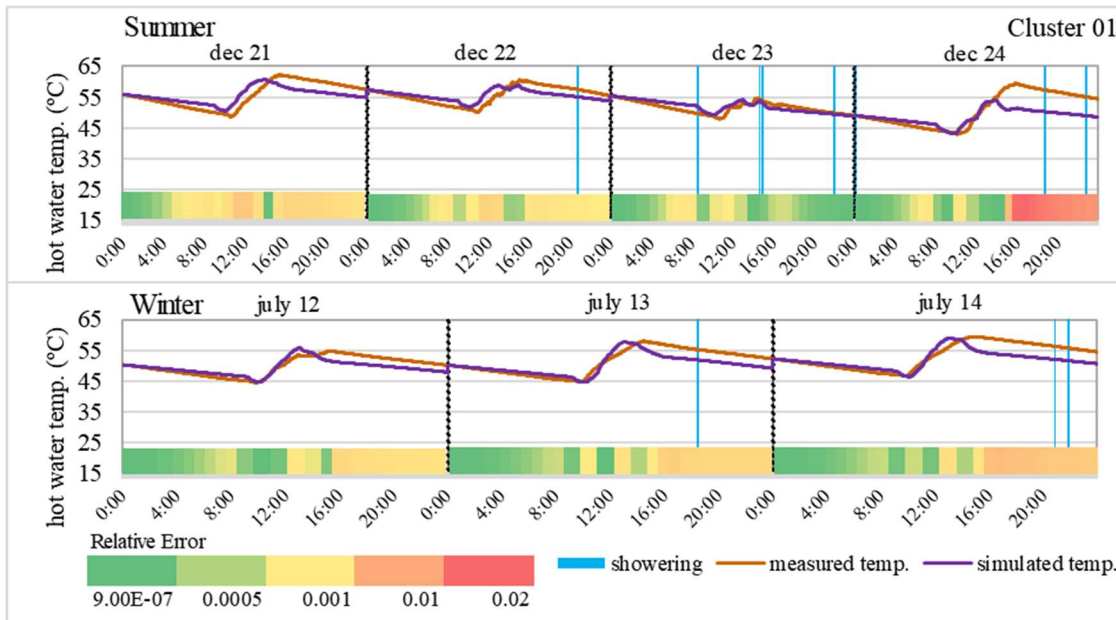
Solar radiation data are solicited by the SizingPeriod:DesignDay object through the indication of schedules of hourly distribution of the direct and diffuse radiation parts in the horizontal plane to each simulated day. Schedules can be created in Schedule:Day:Hourly object. However, according to the data collection process in [7], data of global radiation in the collector’s inclination plan and Paraná Meteorological System (SIMEPAR) were registered, but only for data of global radiation in the horizontal plane. Most Brazilian weather stations monitor global radiation due to sensor acquisition and operation costs. It is necessary to use mathematical models to estimate diffuse and direct radiation parts. Owing to the absence of an hourly correlation model suitable for Londrina, Brazil, this study used the correlation described by Erbs et al. (1982) to calculate the diffuse and direct parts of solar radiation from the data of global radiation in the horizontal plane [9].

RESULTS AND DISCUSSION

Figures 5–9 show the distribution curves of hot water temperatures of each cluster along every validation day with the simulated results and measured data obtained from the monitored solar heating system. The curves of the simulated systems exhibited similar behavior to those of the monitored systems. The same tendency of the inflection points of the water temperature distribution curves was observed. The system simulated for cluster 01 presented the closest similar results to monitoring, where the relative error was maintained less than 0.01 most of the time. However, in

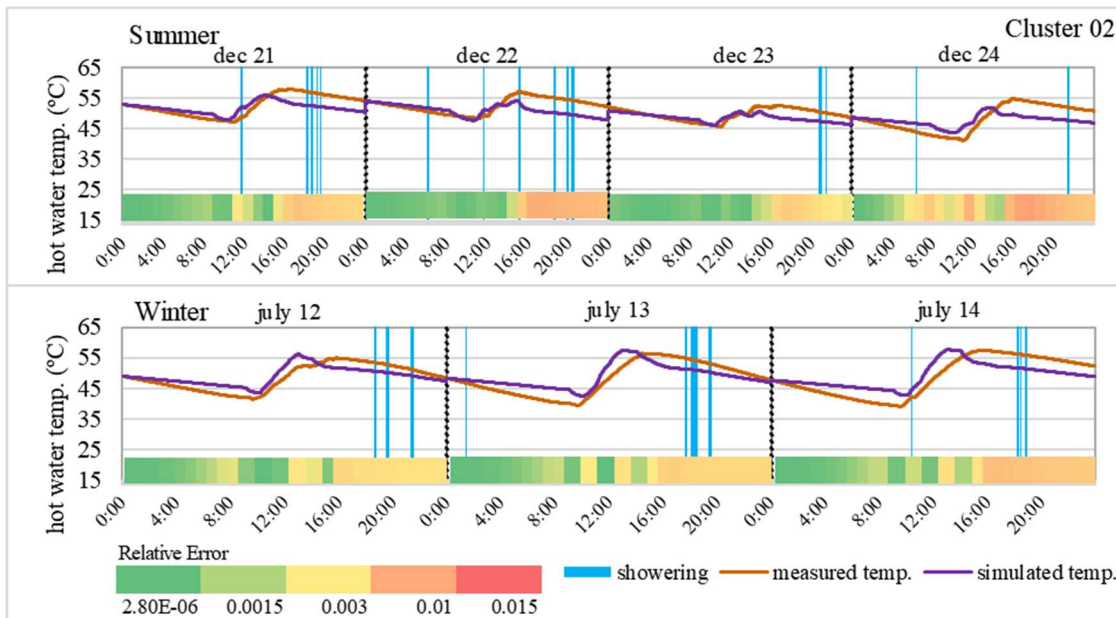
a family of one elderly person and one child, the SWHS was not used several times during winter because of operational difficulties and unfamiliarity with equipment operation. Thus, simulated systems without the interference of user behavior tend to show more accurate results. In the periods of absence of solar radiation in Figures 5–9, before 8 a.m. and after 6 p.m., the simulation curves present the same behavior of the monitored system curves. However, the model tends to underestimate the heat losses during mornings and overestimate them during the evening.

Figure 5: Comparative plots of hot water temperatures on storage tank outlet for summer and winter days – Cluster 01



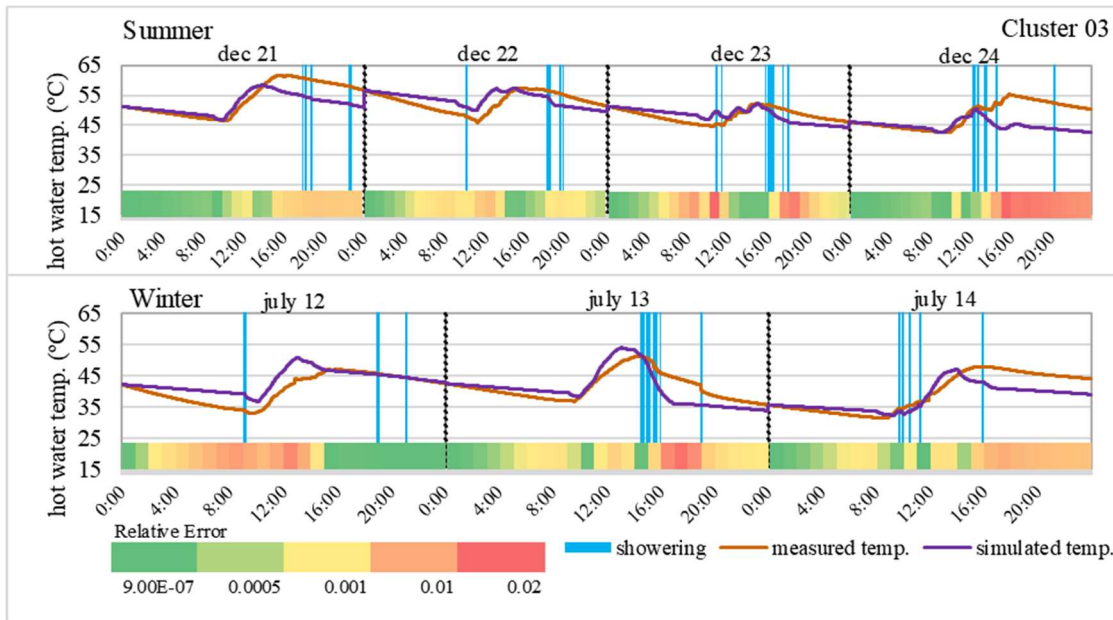
Source: the author.

Figure 6: Comparative plots of hot water temperatures on storage tank outlet for summer and winter days – Cluster 02



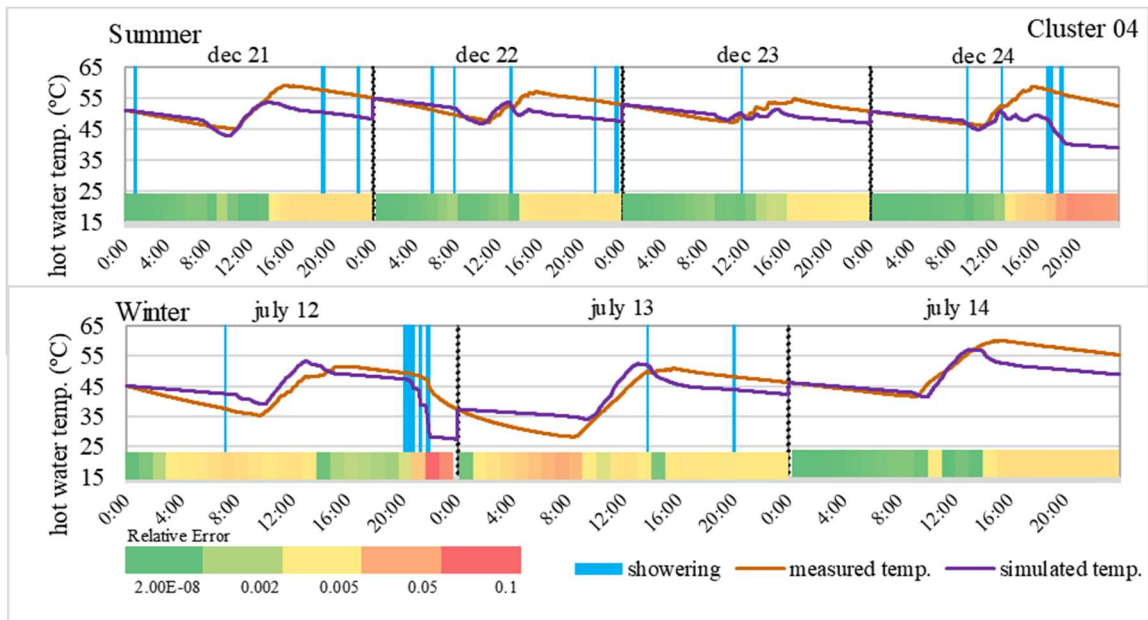
Source: the author.

Figure 7: Comparative plots of hot water temperatures on storage tank outlet for summer and winter days – Cluster 03



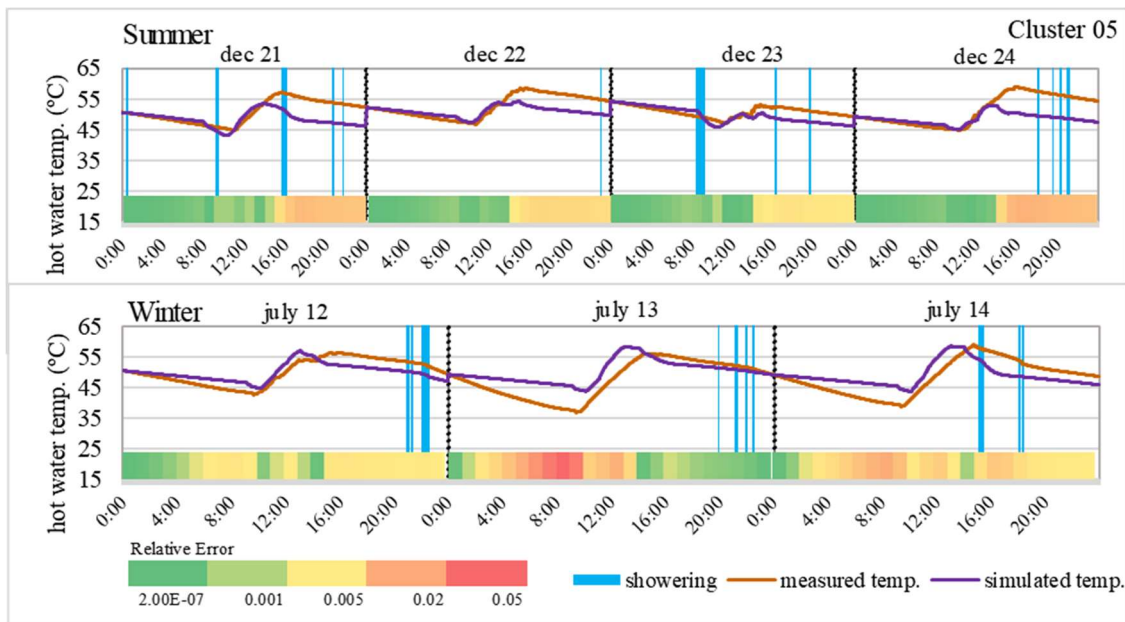
Source: the author.

Figure 8: Comparative plots of hot water temperatures on storage tank outlet for summer and winter days – Cluster 04



Source: the author.

Figure 9: Comparative plots of hot water temperatures on storage tank outlet for summer and winter days – Cluster 05



Source: the author.

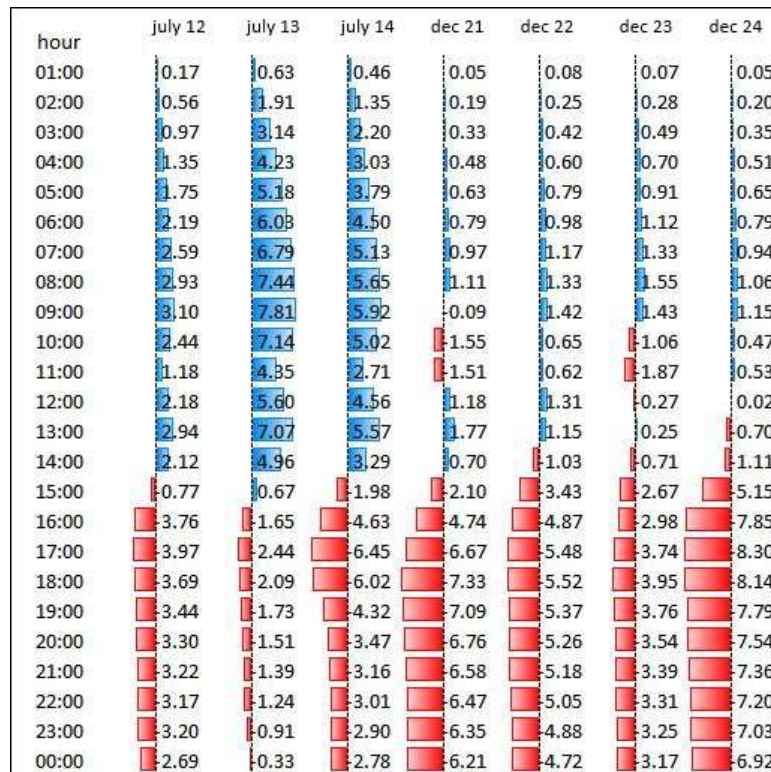
During the period with solar incidence, between 8 a.m. and 6 p.m., different behaviors are observed for summer and winter days. In winter, there is a temporal displacement of the hot water maximum temperature point. The simulated systems present curves with temperature peaks around 2 p.m., while the monitored system temperature peaks occur at 3 p.m. for most clusters. Maximum differences between attained temperatures, although displaced in time, approach an absolute value less than 4 °C in clusters 01 and 02.

In summer, the displacement of the temperature peaks between simulated (3 p.m.) and monitored (4 p.m.) systems occur. However, for all clusters, during summer, the simulated systems do not attain similar temperature peaks. There is a divergence of approximately 15 °C from the monitored system for cluster 04 and 5 °C for cluster 02. The reduced temperature gains and displacement of the simulated system curves when compared with the monitored system can be justified by the non-correspondence of the solar radiation data used in the simulation in comparison with real values. The EnergyPlus software requires solar radiation data fragmented into its direct and diffuse parts. Solely the global radiation could be obtained for Londrina, Brazil, during the validation period. The correlation between the lightness index (kT) and ratio I/I_0 was used to separate global radiation in its direct and diffuse parts. However, these correlations present great variability in the function of the selected temporal partition (hourly, daily, or monthly) of the local and type of adjustment. The correlation reported by Erbs et al. (1982) [9] used in this study results from a statistical analysis of climate data from medium latitude locals, where climate characteristics present lightness conditions distinct from those observed in Londrina, Brazil. When the correlation can calculate the diffuse radiation as a function of the lightness index, the distinction may affect the diffuse fraction values, and therefore, the direct fraction, which is the most important parameter for collector energy gain.

Figure 10 lists the information related to measured and simulated temperatures by presenting the hourly differences of hot water temperature between monitored and simulated systems in absolute value for cluster 05. Positive differences translate the

simulation tendency in super-estimating the measurement, while negative differences indicate that the simulation results underestimate the real data.

Figure 10: Absolute differences between simulated and monitored system for cluster 05, in °C.



Source: the author.

In Figure 10, between 1 a.m. and 8 a.m. of the simulated winter days, a significant tendency of remoteness was observed with an increase in the temperature differences up to 6.8 °C on July 13. In summer days, there was a significant equivalency between the model and monitored system, with a maximum variation of 1.5 °C on December 23. Thus, the model underestimates heat losses in more rigorous climatic conditions, such as in winter. Adjustments in the storage tank heat loss coefficient can help to reduce these differences.

To validate the proposed modeling, the RMSE was used as a statistical metric of the deviation of the modeling results when compared to the SWHS monitored. The results presented in Table 2 are used for the analysis of the RMSE obtained for each cluster and each monitored day. As observed from the measured and simulated temperature distributions in Figure 5, the simulated model for cluster 01 exhibited similar behavior to the monitored system. This is verified by the low RMSE values obtained, which vary between 2.42% and 7.84%, with an overall RMSE of 4.76%. The least RMSE values were obtained for cluster 04, with minimum and dec maximum RMSE equal to 5.56% and 15.14%, respectively, and an overall RMSE of 10.26%. In cluster 04, changes in SWHS during the monitoring period were reported.

Table 2 – Root Mean Square Error for the five clusters

-	Cluster 01	Cluster 02	Cluster 03	Cluster 04	Cluster 05
General RMSE	5.18%	5.97%	7.77%	10.26%	7.53%
Winter RMSE	4.34%	6.65%	8.35%	11.01%	8.43%
Summer RMSE	5.73%	5.41%	7.30%	9.66%	6.78%
RMSE July 12	3.56%	5.07%	8.91	12.30%	5.16%
RMSE July 13	4.21%	6.58%	8.05%	12.23%	10.42%
RMSE July 14	5.10%	7.98%	8.05%	7.93%	8.82%
RMSE December 21	7.14%	4.90%	6.38%	7.83%	7.52%
RMSE December 22	3.63%	5.51%	5.86%	7.18%	5.90%
RMSE December 23	2.42%	4.11%	4.75%	5.56%	4.56%
RMSE December 24	7.84%	6.76%	10.76%	15.14%	8.47%

Source: the author.

It can be observed in Table 2 that, except in cluster 01, the winter RMSE was larger than the summer RMSE. This corroborates the hypothesis that the model underestimates heat losses in more rigorous climate conditions, such as in winter. In cluster 01, the SWHS was rarely used during winter, which explains the low RMSE obtained. There is no consensus regarding a validation method for computer simulations. Many aspects can differ, such as the adoption of different variables, number of validation days, time interval along the day, and statistical metrics for comparison of results. Also, there is no consensus on a maximum value for the RMSE. In this study the strategy of comparison with other similar studies was adopted. When validating a SWHS model simulated in TRNSYS software, [3] obtained a relative error of 4.7% for twenty-five days of simulation. The maximum daily relative error was 21.3%. In [10], a SWHS model with forced circulation was validated; the maximum discrepancies between the modeling and measured system were 20.2%, 16%, and 13.5% for the three output variables observed. The validation of a PVT collector [6] exhibited 2.6% and 8.2% as the relative errors for the electric and thermal efficiencies, respectively.

The performance of the computer modeling obtained in this study was similar to those of the cited studies. For five clusters, the general RMSE varied between 4.76% and 10.26%, and the maximum daily RMSE was 15.14% (for cluster 04, on December 24), which is considered satisfactory in comparison with the results obtained in other studies. The SWHS modeling demonstrated good correspondence with the monitored system for five different usage patterns; however, using a mathematical correlation fitted to Londrina to obtain solar radiation parts may provide further accurate results.

CONCLUSIONS

In this study, the procedures for modeling and validation of a thermosyphon SWHS using the software EnergyPlus was presented. The results show the ability of EnergyPlus in simulating a thermosyphon SWHS under operation as the results obtained via computer modeling corresponded well with the values monitored in five clusters with different system usage.

Consideration of system operation by occupants proved important in model assessment. Comparisons between simulated and measured systems showed that minimum RMSE (4.76%) was obtained for cluster 01, where the occupant presented a lower system usage frequency, particularly in winter. Maximum RMSE (10.26%) was obtained for cluster 04, where changes in SWHS were reported during the monitoring stage. The use of accurate models to simulate thermosyphon SWHSs under operation is fundamental to assess energy saving results obtained when these systems are installed on a large scale in social housing complexes, where M&V techniques are economically not viable.

REFERENCES

- [1] WIT, S., & ALGENBROE, G. Analysis of uncertainty in building design evaluations and its implications. **Energy and Buildings**, v. 34, p. 951-958, 2002. [https://doi.org/10.1016/S0378-7788\(02\)00070-1](https://doi.org/10.1016/S0378-7788(02)00070-1)
- [2] COAKLEY, D., RAFTERY, P., & KEANE, M. A review of methods to match building energy simulation models to measured data. **Renewable and Sustainable Energy Reviews**, v.37, p. 123-141, 2014. <https://doi.org/10.1016/j.rser.2014.05.007>
- [3] KALOGIROU, S., & PAPAMARCOU, C. G. Modelling of thermosyphon solar water heating system and simple model validation. **Energy and Buildings**, v. 21, p. 471-493, 2000. [https://doi.org/10.1016/S0960-1481\(00\)00086-0](https://doi.org/10.1016/S0960-1481(00)00086-0)
- [4] TAHERIAN, H., REZANIA, A., SADEGHI, S., & GANJI, D.D. Experimental validation of dynamic simulation of the flat plate collector in a closed thermosyphon solar water heater. **Energy Conversion and Management**, v. 52, p. 301-307, 2011. <https://doi.org/10.1016/j.enconman.2010.06.063>
- [5] KALOGIROU, S., AGATHOKLEOUS, G., BARONE, A., BUONOMANO, A., FORZANO, C., & PALOMBO, A. A new TRNSYS type for thermosyphon flat-plate solar thermal collectors: validation and optimization procedure. **Renewable Energy**, v.136, p. 632-644, 2019. <https://doi.org/10.1016/j.renene.2018.12.086>
- [6] GUO, C., JI, J., SUN, W., MA, J., HE, W., & WANG, Y. Numerical simulation and experimental validation of tri-functional photovoltaic/thermal solar collector. **Solar Energy**, v. 87, p. 470-480, 2015. <https://doi.org/10.1016/j.energy.2015.05.017>
- [7] GIGLIO, T., & LAMBERTS, R. Savings related to solar water heating system: A case study of low-income families in Brazil. **Energy and Buildings**, v. 130, p. 434-442, 2016. <https://doi.org/10.1016/j.enbuild.2016.08.076>
- [8] GIGLIO, T., SANTOS, V., & LAMBERTS, R. Analyzing the impact of small solar water heating systems on peak demand and on emissions in the Brazilian context. **Renewable Energy**, v. 133, p. 1404-1413, 2019. <https://doi.org/10.1016/j.renene.2018.08.104>
- [9] DUFFIE, J. A., & BECKMAN, W. A. **Solar Engineering of Thermal Processes**. 2. Ed. Nova Iorque: John Wiley & Sons, 2006.
- [10] ABDUNNABI, M. J. R., ALAKDER, K. M. A., ALKISHRIWI, N. A., & ABUGHRES, S. M. Experimental validation of forced circulation of solar water heating systems in TRNSYS. **Energy Procedia** v.57, p. 2477-2486, 2014. <https://doi.org/10.1016/j.egypro.2014.10.257>